JOURNAL OF MATERIALS SCIENCE 28 (1993) 3869–3873

# Influence of vitrification on defect formation during curing of epoxies

YU. A. CHEKANOV, V. N. KOROTKOV, B. A. ROZENBERG, E. A. DHZAVADYAN, L. M. BOGDANOVA
*Department of polymer and composite materials, Institute of Chemical Physics, Russian Academy of Sciences, 142432, Chernogolovka, Moscow region, Russia*

YU. P. CHERNOV, S. G. KULICHIKHIN
*Research Institute of Plastics, 111112, Moscow, Russia*

Defect formation in epoxies due to the chemical shrinkage was observed during isothermal cure over a wide cure temperature range. The observed defects were cohesive cracks and adhesional failures. The influence of the mutual position of the gel and the glass transition points on shrinkage-defect formation was examined. The different types of the cohesive defects can arise in the curing system in both the rubbery and glassy state. The type of defect formed was found to be determined by the relaxational state of the polymer during defect formation. The dependence of the glass transition temperature upon the degree of polymerization is reported for the epoxy/amine polymer system investigated. Experimental parameters of polymer resistance to chemical shrinkage cracking were measured for all investigated cure temperatures.

## 1. Introduction

It is well known that in manufacturing thermoset-based composites residual stresses arise, which can adversely affect the mechanical properties of the material. Many experimental works have been devoted to investigation of the influence of different factors on the internal stresses. Abibov and Molodtzov [1] examined the residual stresses in a simple experimental model of the composite using a photoelastic technique. The model involved an outer glass tube treated on the inside with an anti-adhesive in which four steel fibres were placed and cast in polymer. The influence of chemical shrinkage and the difference between the thermal expansion coefficients of the matrix and reinforcement upon stress distribution was investigated in the present work. The contribution of the latter factor to the residual stress value is considerably more than that of chemical shrinkage. Sarabeev and Perlin [2] gave a characterization of the volume stress distribution for a similar model with glass fibres using the same technique, but in contrast to the previous investigation, the tube treatment resulted in good adhesional connection with polymer. The same authors also demonstrated the large influence of apprets on internal stress distribution [3]. This experimental model was improved by Cunningham *et al.* [4] and the number of glass fibres used was 10–12. The internal stress distribution arising after curing and cooling from the cure temperature to room temperature, was also examined by the latter authors. Shimbo *et al.* investigated the internal stresses, with the aid of a two-dimensional model using the strain gauge method. Shrinkage and temperature stresses were found to increase with increasing cure conversion and glass transition temperature, $T_g$, of the cured system. Srivastava and White determined the curing stresses in polymer sheets using the layer removal procedure. The lower isothermal cure temperature and the lower residual stress level were found. Thus some relationships between technological factors and internal stresses have already been determined.

The comparison of the internal stress value with the material strength must be the next step of the investigation in order to determine whether or not the internal stresses can lead to material cracking. However, strength measurements during the manufacturing of composites are, as a rule, rather difficult, and we cannot compare the stress value with the material strength in many cases, because the latter value is unknown. However, if defects arise in the composite we can confirm that the internal stress value exceeds the material strength. For instance, Cooper and Sillwood [7] found defects to arise in a composite under thermal stresses. Thus, composite cracking during the fabrication process can also be used as a technological criterion. However, to evaluate the defect quantity in the composite is rather difficult; therefore to utilize experimental composite models and to examine defect formation in these are probably more convenient and reliable methods.

A simple technique was proposed earlier [8, 9] for the investigation not only of the shrinkage stresses, but also of shrinkage defects. In order to observe defect formation, cylindrical glass tubes were filled with uncured epoxy system, so there was a good adhesional connection of polymer with the rigid tube

0022–2461  

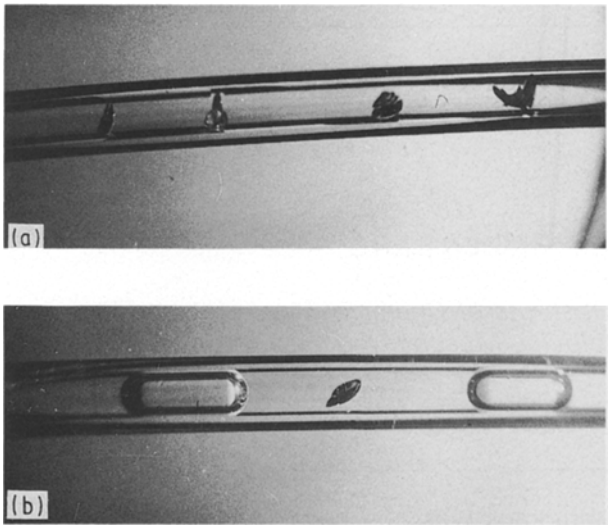


*Figure 1* Polymer specimens to determine parameters (a) $\bar{l}$, and (b) $\bar{L}_{min}$, with shrinkage cracks. Cure temperature 90 °C.

walls. The defects arose in the polymer during isothermal curing as cohesive cracks and adhesional failures. Two parameters were used by Korotkov *et al.* [9] to characterize the polymer resistance to the cohesive defect formation; (1) $\bar{l}$, the mean relative distance between cracks which is equal to the mean distance between cohesive cracks (Fig. 1a) in long specimens, divided by the inner tube diameter; and (2) $\bar{L}_{min}$, the length of the minimal damaged polymer specimen contained between air-gaps inside the glass tube (Fig. 1b). Greater values of these parameters correspond to a higher resistance of curing matrix to shrinkage cracking. The previous investigation [9] was carried out at cure temperatures higher than the glass transition temperature of completely cured polymer, $T_{g,\infty}$. In this particular investigation, the cure temperatures were lower than $T_{g,\infty}$, therefore in all experiments, vitrification took place during the isothermal cure [10] ($T_{cure} < T_{g,\infty}$). This fact greatly complicates the observed phenomena. To elucidate the influence of vitrification of isothermally cured epoxies on the character of shrinkage-defect formation was the main object of the present work.

## 2. Experimental procedure

Glass capillaries with an inner diameter of 1.6 mm were used, therefore each polymer specimen had two free surfaces, upper and lower ones, in vertical capillaries. Epoxyamine composition diglycidyl ether of resorcinol, DGER, and *m*-phenylenediamine, m-PhDA in stoichiometric ratio of epoxide groups to NH was used for the investigation. The epoxide equivalent weight (EEW) of DGER was 122 g eq$^{-1}$ (EEW = 111 g eq$^{-1}$ for the pure chemical). The amine equivalent weight (AEM) of *m*-PhDA was 54 g eq$^{-1}$ (AEM = 54 g eq$^{-1}$ for the pure chemical). The initial substances were in the crystalline state. DGER was melted at 40 °C, and then *m*-PhDA was added and stirred for 10 min. Then the homogeneous liquid epoxy system was degassed under vacuum for a further 10 min. The quantity of reacted epoxy groups in the composition after the preparation procedure was determined by chemical analysis and was equal to 4%–6%.

Four routine techniques were also used apart from the technique of the determination of parameters $\bar{l}$ and $\bar{L}_{min}$. Isothermal calorimetry at different temperatures was used to ascertain the chemical kinetic curves. To calculate epoxy group conversion, the enthalpy of the epoxy cycle opening was supposed to equal 25 kcal mol$^{-1}$ [11]. A steady shear cone-and-plate Rheotest-2 was utilized to determine the isothermal rheological behaviour of the system investigated (shear rates 900–0.5 s$^{-1}$). An MK-3 device (USSR) was used to record the isothermal torsional braid analysis (TBA) traces (frequency $\simeq$ 1 Hz).

### 2.1 Thermomechanical measurements

Thermomechanical analysis (TMA) of the polymer samples was used for the determination of $T_g$. Specimens for TMA were cured in an oven simultaneously with polymer samples used for determination of parameters $\bar{l}$ and $\bar{L}_{min}$. The former specimens were removed one after another from the oven during the isothermal cure, then the conversion of all the TMA specimens removed was determined from known isothermal chemical kinetics. The TMA specimens isothermally cured at temperatures of 40–150 °C were tested at a heating rate of 2.5 °C min$^{-1}$, 300 gm load and stick diameter of 1.78 mm. In order to improve accuracy of measurement, the TMA specimens cured at 20 °C were tested at a heating rate of 1.25 °C min$^{-1}$, 50 gm load and stick diameter of 1.78 mm. The dependence of $T_g$ on the degree of polymerization is presented in Fig. 2 (the conversion was calculated taking into account that 5% epoxy groups had reacted during the preparation procedure). With the aid of this dependence, the moment of vitrification was determined for all isothermal cure experiments. The experimental dots were fitted using Di Benedetto's equation [12]

$$\frac{T_g - T_g^\circ}{T_g^\circ} = \frac{(E_x/E_m - F_x/F_m)X}{1 - (1 - F_x/F_m)X} \quad (1)$$

where $T_g^\circ$ is glass transition temperature of an unreacted mixture, $E_x/E_m$ is the ratio of lattice energies for cross-linked and uncross-linked polymer, $F_x/F_m$ is the corresponding ratio of segmental mobilities and $X$ is the extent of conversion at the glass transition. The values of the parameters calculated by fitting are $T_g^\circ = -39$ °C, $E_x/E_m = 0.19$, $F_x/F_m = 0.11$.

## 3. Results and discussion

Experiments to observe the defect formation were carried out over a wide temperature range from 5–100 °C. It is possible, conventionally, to distinguish three temperature ranges, in each of which a certain consequence of the phenomena and the type of defect occurs.

### 3.1. High-temperature range

In Range I the investigated temperatures were 70–100 °C (see Fig. 3). In these experiments there were

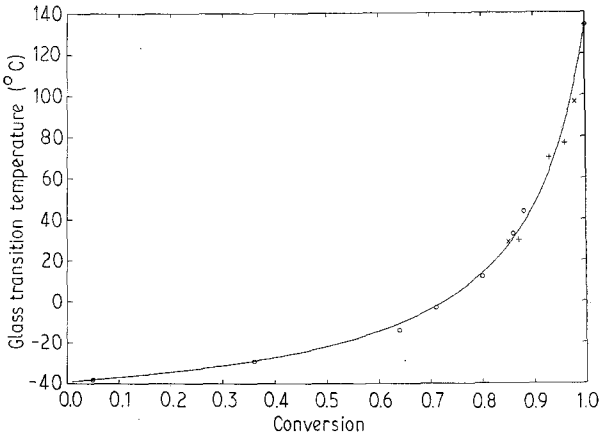


*Figure 2* The dependence of $T_g$ on conversion. Relative cure temperature of TMA specimens; (○) 20 °C, (+) 60 °C, (×) 80 °C, (●) 150 °C.

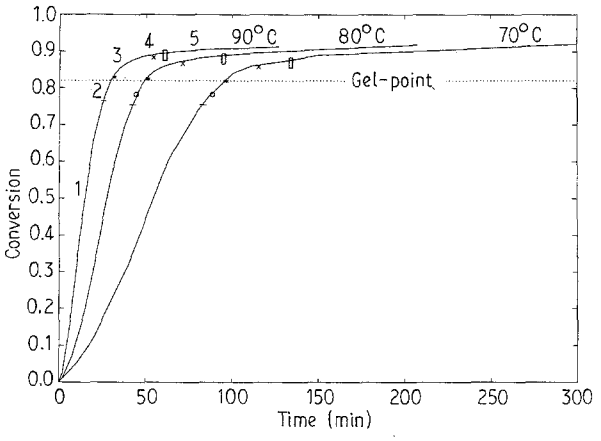


*Figure 3* The curing kinetics at 70, 80 and 90 °C. (1–5) The five observable stages. (−) Cessation of flow, (○) onset of void appearance, (*) appearance of first cohesive defects, (×) end of defect formation, (□) vitrification of the polymer ($T_g = T_{cure}$).

no visible changes during the first stage of cure, except for a movement of both menisca to the centre of the specimen due to chemical shrinkage. The polymer remained liquid during the first stage. At the beginning of the second stage, the resin ceased to flow in the tilted glass ampoule with an inner diameter of 4 mm. The cessation began at approximately the same value of conversion (near 77%) at all temperatures, indicating that the curing system is in the pre-gel state and soon turns from the liquid into a highly elastic state. Movement of the menisca is not due to the high viscosity of the polymer in this stage, and the maximal tensile stresses arise in the centre of the specimen. These stresses result in void formation (Fig. 4): the formation of voids rather than flat cracks indicates that the polymer is still liquid. The subsequent formation of cohesive cracks, Fig. 5, at the beginning of Stage 3, is evidence that the polymer becomes a highly elastic body, i.e. the curing system has reached the gel-point. The cohesive cracks in the third stage at all temperatures have a similar appearance. They are randomly oriented and have an uneven surface. Their lengths do not exceed one or two times the inner diameter of the tube along the axis of the tube, and are

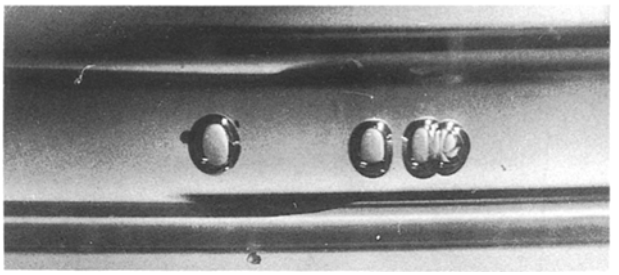

*Figure 4* Voids arising in the polymer during isothermal curing immediately prior to gelation. Cure temperature 80 °C.

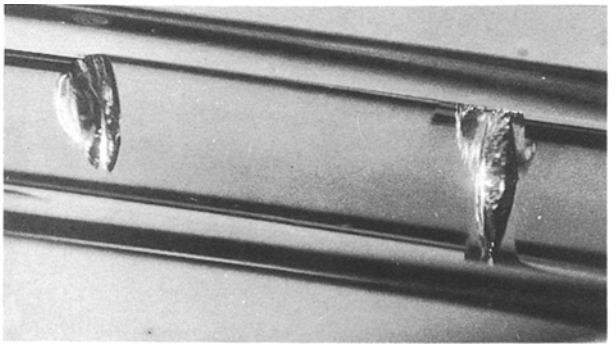

*Figure 5* Shrinkage cohesive cracks. Cure temperature 90 °C.

similar to relative defect lengths described elsewhere [9]. Cure conversion, when shrinkage defects occur in the form of cohesive cracks, is about 82%–84% for the different temperatures in Range I.

Measurements of viscosity and the TBA trace show (Fig. 6) gelation to take place in the investigated system at the same degree of conversion. Gel-time, determined from viscosity, $\eta$, measurement, as the time at which $1/\eta \to 0$, is 29 min and the degree of polymerization reached for this time is 82% ($T_{cure} = 90$ °C). The first TBA peak corresponds to a time of 25 min and a conversion of 78%. Enns and Gillham assigned [13] the mechanical loss tangent ($\tan\delta$) peak, occurring immediately prior to the vitrification peak, to gelation, but Stutz and Mertes [14] have shown that this peak precedes gelation and corresponds to isoviscous phenomena. In our case, the first TBA peak also precedes gelation as detected by viscosimetry. The coincidence of degrees of conversion of the cohesive defect origin, and direct measurements of the gel-point, shows that the former phenomenon can be used as an indication of the gelation in the curing system considered. The second TBA peak time is 55 min and this result is in a good agreement with the vitrification time detected in thermomechanical measurements, which was 60 min.

New defects continue to arise for some time. The dangerous conversion zone, when defects arise, is much longer at higher temperatures. As seen from Fig. 3, it is about 5% for 90 °C, and 3% for 70 °C. The following reasons can explain the difference in duration of the dangerous interval at different temperatures. Because the onset of the cohesive defect formation is practically the same in all cases and, as discussed above, it coincides with the gelation of the

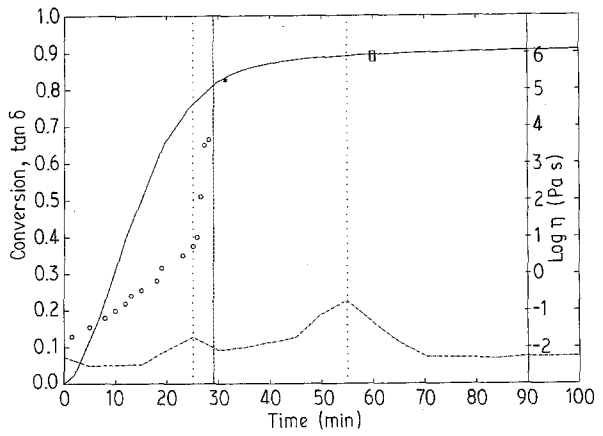


*Figure 6* (—) Kinetics of cure, (○) viscosity, and (—·—) TBA trace at 90 °C. Vertical dotted lines indicate maxima of tan $\delta$. Vertical dashed line indicate the moment at which $1/\eta \rightarrow 0$. (*) Appearance of first cohesive defects, (□) vitrification of the polymer detected by thermomechanical measurements.

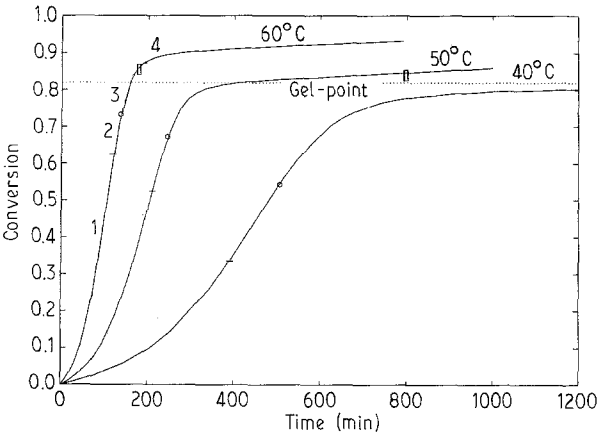


*Figure 7* The curing kinetics at 40, 50 and 60 °C and four observable stages. (—) Cessation of flow, (○) onset of the void appearance, (□) vitrification of the polymer ($T_g = T_{cure}$).

system for the different temperatures, the moment at which defect formation ceases will determine the duration of the dangerous interval. It will also be shown that the vitrification suppresses the defect formation in temperature range I. At higher temperatures, vitrification occurs at a greater degree of conversion [10]. Therefore, completion of the cracking is displaced to higher conversions, leading to an extension of the dangerous conversion zone. The cohesive cracks and the voids are taken into account for calculation of the parameter $\bar{l}$, because they both damage the samples and their influence on the surrounding material is identical from the viewpoint of tensile stress distribution [9].

The moment at which defect formation is completed (the beginning of Stage 4) and the moment at which vitrification of the system occurs (the beginning of Stage 5), determined from the thermomechanical measurements, are very close. This points to their possible correlation which is probably caused by an increase in the polymer strength due to vitrification. The conversion zone of Stage 4 for higher temperatures is shorter than for lower temperatures. For example, for 90 °C it is 1%, but for 70 °C it is 3%. The main peculiarity of this stage is that the polymer is in the pre-glassing state. This is decisive for termination of defect formation.

Vitrification of the sample indicates the onset of Stage 5. No defects arise in this stage, although the cure reaction additionally develops by approximately 4%–6%.

## 3.2. Intermediate temperatures

The main peculiarity of temperature Range II (40–60 °C) is that no cohesive defects occurred at these temperatures (Fig. 7). The initial development of events is identical to that of Range I, but in distinction from Range I the onset of the cessation of polymer flow is different at the different temperatures. The flow of the curing system ceases at lower conversions for the lower temperatures in Range II (the beginning of Stage 2). Voids then occur in the curing system (the beginning of Stage 3). Some time after that moment, the curing system is gelled and at once vitrifies (the beginning of Stage 4). The appearance of the voids changes at this stage and the void surface becomes uneven. From Fig. 7 vitrification can be seen to take place at approximately the same conversion as gelation. Therefore, the polymer is not in the highly elastic state after gelation as it was in Range I, but is in the pre-glassing state. Owing to this, crack formation is completely suppressed. The parameter $\bar{l}$ is calculated by taking into account only the voids with an uneven surface, because no other defects occur in Range II (Fig. 8).

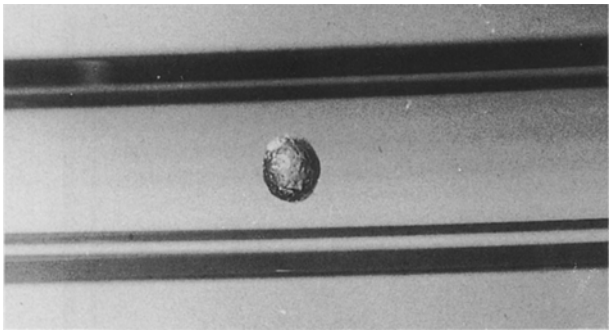

*Figure 8* Final appearance of a shrinkage defect in Range II of the cure temperatures.

## 3.3 Low temperatures

Temperature Range III (5–20 °C) is more complex, because the cure reaction lasts some days (Fig. 9). In this temperature region, calorimetric measurements of the cure kinetics were made using the following procedure. The epoxy was cured at the chosen temperature for different times, $t$, and then post-cured at 90 °C. The cure conversion was calculated using the formula

$$\alpha(t) = (\alpha_\infty^{90\,^\circ C})_0 - (\alpha_\infty^{90\,^\circ C})_t$$

where $\alpha_\infty^{90\,^\circ C}$ is residual conversion during post-cure, indexes 0 and $t$ denote the curing time at the temperature investigated before post-cure measurements.

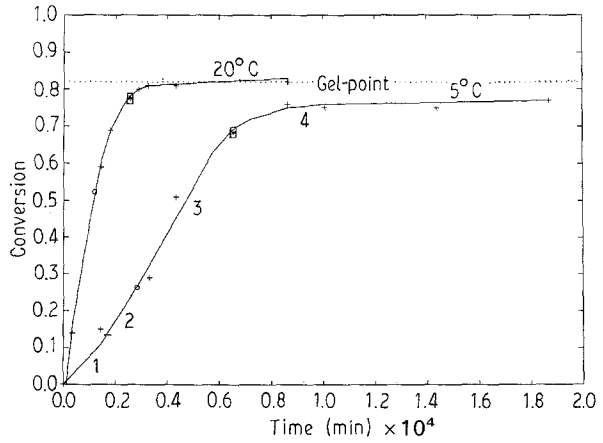


*Figure 9* The curing kinetics at 5 and 20 °C and four observable stages. (—) Cessation of flow, (○) onset of void appearance, (*) appearance of first cohesive defects, (□) vitrification of the polymer ($T_g = T_{cure}$), ( + ) experimental points.

The liquid state exists over quite a short conversion interval in Range III (Stage 1). The flow of the curing system stops at a conversion equal to 15% at $T_{cure} = 5\,°C$ (the beginning of Stage 2). Then voids arise and grow (Stage 3). When the curing system vitrifies the appearance of the failures changes, and new cohesive cracks with a smooth surface are seen. The appearance of these cracks differs strongly from that of cohesive cracks in temperature Range I, and the surface of the cracks is smooth, as distinct from the uneven surface of the cracks in Range I. Moreover, Range III cracks propagate along the polymer specimen crossing in a zig-zag path from one wall to the other (Fig. 10). It is not possible to calculate parameter $\bar{l}$, because it is very difficult to distinguish the individual cracks. We can only confirm that the value of $\bar{l}$ is very small, because, in fact, there are many cracks in the sample.

It should be noted that vitrification takes place earlier than the gelation, as distinct from Range II. This is the main reason for crack formation in the glassy state in Range III and the absence of cracks in Range II.

## 4. Conclusions

The values of the characteristic parameters $\bar{l}$ and $\bar{L}_{min}$ of the shrinkage defects formed in different temperature ranges are given in Fig. 11.

On analysing the above-mentioned phenomena, we can draw the following conclusions concerning the influence of vitrification on defect formation during isothermal curing of a three-dimensionally constrained thermoset system.

1. The cure temperature drastically affects shrinkage defect formation.

2. Such defects can arise in the curing systems both in the rubbery and glassy states.

3. The type of defects formed is determined by the relaxational state of the polymer during defect formation.

4. The influence of vitrification on defect formation is quite different in the different temperature ranges. Virtrification suppresses defect formation when gelation of the curing system precedes its vitrification, or

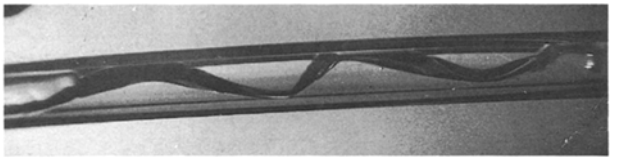

*Figure 10* Zig-zag-like shrinkage defect observed in cure temperature Range III.

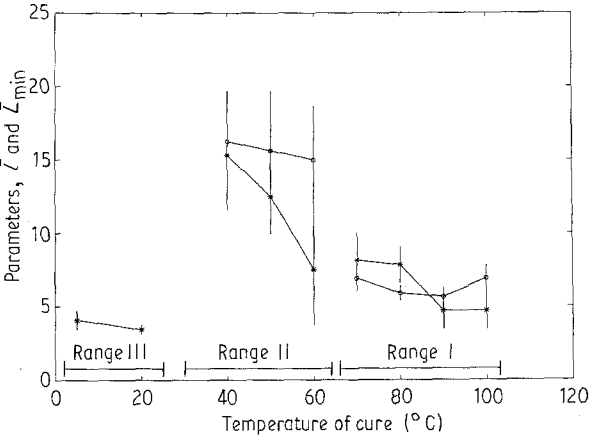


*Figure 11* Dependence of parameters $\bar{l}$ and $\bar{L}_{min}$ on the cure temperature: (*) $\bar{L}_{min}$ and (○) $\bar{l}$ calculated as mean root square values with mean square error.

especially when they occur at the same degree of conversion, but it promotes crack formation when vitrification precedes gelation.

5. From the technological point of view, temperature Range II attracts an attention, because the number of defects is minimal in this range. Thus shrinkage crack formation can be minimised in the cured composites by careful choice of cure regime.

## Acknowledgements

The authors thank E.E. Al'yanova for help with thermomechanical measurements and G.S. Zaspinok for the photography.

## References

1. A. L. ABIBOV and G. A. MOLODTZOV, *Mech. Polym. (USSR)* (1965) 76.
2. V. F. SARABEEV and S. M. PERLIN, *ibid.* (1973) 661.
3. *Idem, ibid.* (1974) 43.
4. B. CUNNINGHAM, J. P. SARGENT and K. H. G. ASHBEE, *J. Mater. Sci.* **16** (1981) 620.
5. M. SHIMBO, M. OCHI and Y. SHIGETA, *J. Appl. Polym. Sci.* **26** (1981) 2265.
6. A. K. SRIVASTAVA and J. R. WHITE, *ibid.* **29** (1984) 2155.
7. G. A. COOPER and J. M. SILLWOOD, *J. Mater. Sci.* **7** (1972) 325.
8. A. R. PLEPYS and R. J. FARRIS, *Polymer* **31** (1990) 1932.
9. V. N. KOROTKOV, Yu. A. CHEKANOV and B.A. ROZENBERG, *J. Mater. Sci. Lett.* **10** (1991) 896.
10. G. WISANRAKKIT and J. K. GILLHAM, *J. Appl. Polym. Sci.* **41** (1990) 2885.
11. B. A. ROZENBERG, *Adv. Polym. Sci.* **75** (1985) 113.
12. A. T. Di BENEDETTO and L. E. NIELSEN, *J. Macromol. Sci. Rev. Macromol. Chem.* **C3** (1969) 69.
13. J. B. ENNS and J. K. GILLHAM, *J. Appl. Polym. Sci.* **28** (1983) 2567.
14. H. STUTZ and J. MERTES, *ibid.* **38** (1989) 781.

*Received 17 March*
*and accepted 21 October 1992*